

# Domain Adaptation based Fault Diagnosis under Variable Operating Conditions of a Rock Drill

Yong Chae Kim<sup>1</sup> , Taehun Kim<sup>1</sup> , Jin Uk Ko<sup>1\*</sup> , Jinwook Lee<sup>1</sup> , and Keon Kim<sup>1,2</sup> 

<sup>1</sup>*Department of Mechanical Engineering, Seoul National University, Seoul, 08826, Republic of Korea*

*313nara@snu.ac.kr  
crown3633@snu.ac.kr  
coolstyle@snu.ac.kr  
ljw723@snu.ac.kr*

<sup>2</sup>*Hyundai Doosan Infracore Inc., Incheon, 22502, Republic of Korea*

*keon.kim2@hyundai-di.com*

## ABSTRACT

Data-driven fault diagnosis is an essential technology for the safety and maintenance of rock drills. However, since the signals acquired from a rock drill have different distributions, which arise due to their variable operating conditions, the classification performance of any data-driven method is diminished; this is called the domain-shift issue. This paper proposes a new domain-adaptation-based fault diagnosis scheme to solve the domain-shift problem. The proposed method introduces a data-cropping technique to mitigate the difference in the length of the data measured from a rock drill for each impact cycle. To extract invariant features for all operating conditions, the proposed method combines two methods: a domain adversarial neural network and minimization of the maximum mean discrepancy (MMD) between the features from different domains. In addition, a soft voting ensemble is used to reduce the model uncertainty. The proposed method shows superior performance when validated with a rock drill dataset; the proposed approach was ranked in 2<sup>nd</sup> place in the 2022 PHM Conference Data Challenge.

## 1. INTRODUCTION

A rock drill operates under harsh environmental conditions that include vibration and moisture (Erik, Erik, Mattias, & Robert, 2021). Operating a rock drill under these harsh conditions makes it vulnerable to various uncertainties that might be detrimental to the health state of the machinery. Therefore, diagnosing the health condition of a rock drill is very important for safety and maintenance. Recent advances

in sensor technology have made it possible to obtain vast amounts of data. Deep-learning-based fault diagnosis using the large amount of data available for various mechanical systems is widely investigated. Li, Chow, Tipsuwan, and Hung (2006) proposed a neural network that uses frequency characteristic features to diagnose bearings in a motor. In other work, Guo, Chen, and Shen (2016) proposed a hierarchical adaptive deep convolutional neural network (ADCNN) to classify bearing faults. ADCNN achieved high accuracy through automatic feature extraction.

Although deep-learning-based fault-diagnosis approaches show excellent performance, the previously proposed algorithms assume that the training data and the test data share the same distribution. However, mechanical systems that operate in real industrial fields do not satisfy this assumption. When the operating conditions change, the data distributions also change considerably; this is called the domain-shift issue. In an effort to minimize the large domain shift observed in real-world settings, adversarial learning has been adopted; this approach was initially developed in the computer vision field (Ganin, Ustinova, Ajakan, Germain, Larochelle, Laviolette, Marchand, & Lempitsky, 2016). Fault diagnosis through adversarial learning has been widely studied as a way to handle the large domain-shift problem. Jiao, Zhao, and Lin (2019) proposed an adversarial adaptation network based on classifier discrepancy (AACD) to diagnose planetary gearboxes. Guo, Lei, Xing, Tan, and Li (2018) developed a deep convolutional transfer learning network (DCTLN). DCTLN allows learning of domain-invariant features using a domain adversarial neural network and maximum mean discrepancy (MMD).

In this paper, we propose a new fault-diagnosis algorithm to solve the domain-shift problem of a rock drill that operates under variable operating conditions. The proposed method introduces a data-cropping technique to mitigate the issue

Yong Chae Kim et al. This is an open-access article distributed under the terms of the Creative Commons Attribution 3.0 United States License, which permits unrestricted use, distribution, and reproduction in any medium, provided the original author and source are credited.

\*Corresponding Author: Jin Uk Ko (coolstyle@snu.ac.kr)

<https://doi.org/10.36001/IJPHM.2023.v14i2.3425>

that arises because the length of each dataset is different. In addition, the proposed algorithm uses an adversarial learning approach to extract domain-invariant features and metric learning to reduce the distribution discrepancy.

The main contributions of the proposed method are as follows:

1. The proposed method developed a data-cropping preprocessing technique using physical knowledge of a hydraulic rock drill.

2. The proposed method performs multi-source domain adaptation by combining the existing MMD loss and adversarial loss.

3. The proposed model can reduce the uncertainty in the classification by using the soft voting ensemble technique.

The rest of this paper is organized as follows. In Section 2, we introduce the problem to be solved. The proposed method is explained in detail in Section 3; the verification results are presented in Section 4. Finally, the conclusion is summarized in Section 5.

## 2. PROBLEM DESCRIPTION

The proposed algorithm in this paper was developed for the 2022 PHM Conference Data Challenge. The problems and datasets described in Section 2 are the same as those introduced in the description of the data challenge.

### 2.1. Data Description

The data used in the algorithm were obtained through a testbed experiment in a laboratory environment. Data was measured by attaching a total of three sensors (pin, pdin, po); the sampling frequency of the sensors was 50 [kHz]. A description of each sensor is shown in Table 1. There are eleven conditions, including one normal condition and ten fault conditions. The definition of each health condition is shown in Table 2. The locations of the sensors and the faults are described in Figure 1. All data are divided into impact cycle units and are normalized for each impact cycle.

Sensor	Sampling	Description
pin	50kHz	Percussion pressure at inlet fitting
pdin	50kHz	Damper pressure inside the outer chamber
po	50kHz	Pressure in the volume behind the piston

Table 1. Pressure sensor names and descriptions.

Label	Letter	Description
1	NF	No-fault
2	T	Thicker drill steel
3	A	A-seal missing. Leakage from high pressure channel to control channel.

4	B	B-seal missing. Leakage from control channel to return channel.
5	R	Return accumulator, damaged
6	S	Longer drill steel
7	D	Damper orifice is larger than usual
8	Q	Low flow to the damper circuit
9	V	Valve damage. A small wear-flat on one of the valve lands.
10	O	Orifice on control line outlet larger than usual
11	C	Charge level in high-pressure accumulator is low

Table 2. Fault class of the rock drill dataset.

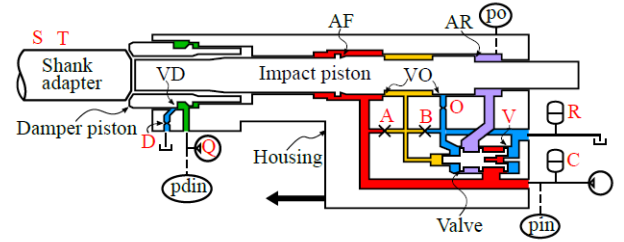


Figure 1. Locations of the sensors and faults.

### 2.2. Problem Definition

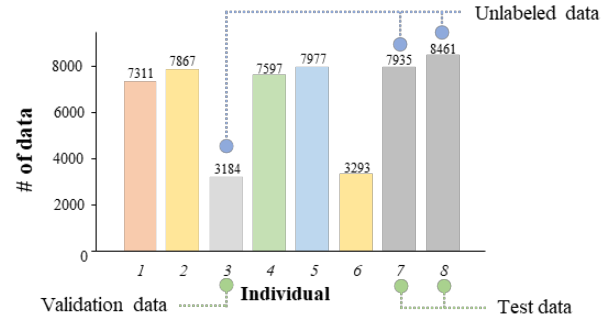


Figure 2. The number of samples in each individual dataset.

The total dataset includes data measured under eight different operating conditions; these data are expressed as individual datasets. The number of samples in each individual dataset is shown in Figure 2. Each individual dataset has a different number of data, and the number of conditions for each individual dataset is similar but slightly different. Datasets 1, 2, 4, 5, and 6 are used as the training dataset, and sets 3, 7, and 8 are unlabeled data; they are utilized for the validation and test data. We define the training dataset as source data  $\mathcal{D}_s = \{\chi_s, y_s\}$  and the validation/test dataset as target data  $\mathcal{D}_t = \{\chi_t\}$ . Each dataset has a different impact cycle; the data contains a total of eleven conditions, including one normal and ten fault conditions.

Accuracy is used as the evaluation metric. The mathematical definition of accuracy is as follows:

$$Accuracy = \frac{TP + TN}{TP + TN + FP + FN} \quad (1)$$

*TP: True positive*

*TN: True negative*

*FP: False positive*

*FN: False negative*

### 3. PROPOSED METHOD

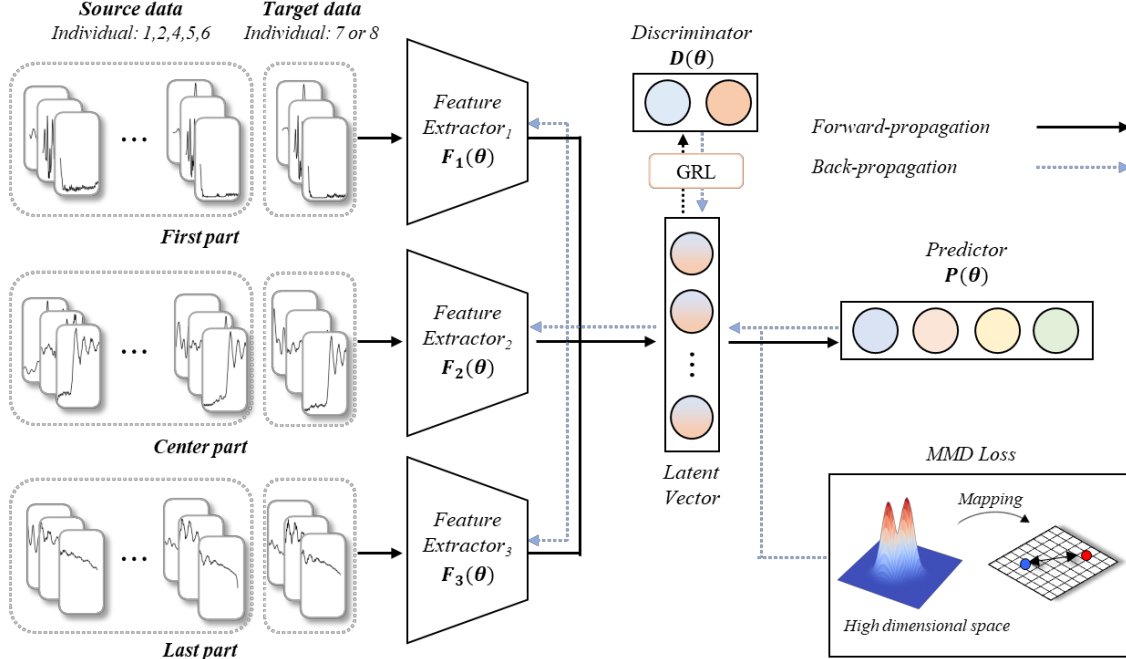


Figure 3. Configuration of the proposed method.

The proposed method is described in this section. Considering that a rock drill operates under various operating conditions, a new fault-diagnosis approach is proposed in this work to decrease the domain discrepancy that arises in varying conditions. Figure 3 shows the overall configuration of the proposed method. First, a data cropping technique is employed to mitigate the issue of the different lengths of the impact cycle of the rock drill. The proposed algorithm uses an adversarial learning scheme to extract domain-invariant features and MMD to reduce the distribution discrepancy. The loss function of the proposed method consists of three loss terms: task classification loss ( $\mathcal{L}_y$ ), domain classification loss ( $\mathcal{L}_D$ ), and MMD loss ( $\mathcal{L}_{MMD}$ ). The proposed loss function is defined as follows:

$$\mathcal{L} = \mathcal{L}_y + \alpha \mathcal{L}_D + \beta \mathcal{L}_{MMD} \quad (2)$$

where  $\alpha$  is the penalty parameters for the domain classification loss function, and  $\beta$  is the penalty parameters for the MMD loss function.

#### 3.1. Data Preprocessing

Figure 4 presents one impact cycle for the normal condition. The impact cycle shows different patterns in the first, middle, and last three parts. In a hydraulic rock drill, three processes of rearward acceleration, retardation, and forward acceleration occur sequentially during one impulse. Forward acceleration occurs at the beginning of the data, retardation occurs at the middle, and forward acceleration occurs at the end (Erik, Erik, Mattias, & Robert, 2021). Thus, the proposed method cropped the three parts to include the physical knowledge of the hydraulic rock drill. The maximum length is 900 and we set the size of each part as 300 to use all data points. Since it has three sensors, preprocessing is performed for each sensor. Therefore, as described in Figure 5, the dimension of the data becomes [3,3,300] for one impact cycle. The proposed method employs a convolutional neural network (CNN) as a feature extractor (FE) and the channel is determined according to the number of sensors. In addition,

the number of extractors is determined by the number of preprocessed crops. Since the proposed method consists of the first, center, and last parts, three extractors are used. Therefore, each extractor selects an important feature, according to the location of the data point.

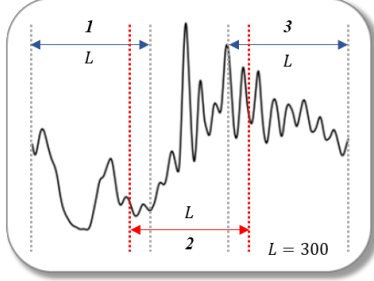


Figure 4. Data preprocessing of the proposed method.

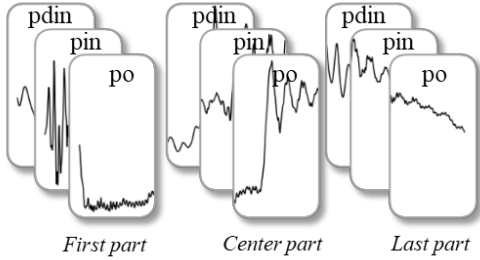


Figure 5. The input data of the proposed method.

### 3.2. Domain Adversarial Neural Network

An adversarial learning scheme is proposed for a generative adversarial network (GANs). It is graphically described in Figure 6. In the figure, green denotes backpropagation with a negative value, and red indicates backpropagation with a positive value. The scheme makes the generator and the discriminator compete with each other. Inspired by this, a domain adversarial neural network (DAAN) is used, in which the adversarial learning method confuses source data ( $\mathcal{D}_s$ ) and target data ( $\mathcal{D}_t$ ) for the extractor to extract domain-invariant features. The loss function of DANN is defined as:

$$\mathcal{L}_{DANN} = \mathcal{L}_y + \alpha \mathcal{L}_D \quad (3)$$

$$\mathcal{L}_y = -\frac{1}{m^s} \sum_{i=1}^{m^s} y_i \log \hat{y} \quad (4)$$

$$\mathcal{L}_D = -\frac{1}{m^s + m^T} \sum_{i=1}^{m^s + m^T} d_i \log \hat{d} \quad (5)$$

where  $m^s$  is the number of the source domains,  $m^T$  is the number of the target domain,  $y$  is the class label,  $\hat{y}$  is the predicted class label,  $d$  is the domain label, and  $\hat{d}$  is the predicted domain label. In Eq. (4), a task classification loss is used to classify the classes well; The domain classification loss is used to discriminate the domains in Eq. (5). The loss

is backpropagated for the predictor and domain discriminator to distinguish the class and domain well. In the extractor, the task classification loss is backpropagated as it is; however, the domain classification loss is backpropagated through the gradient reversal layer (GRL) because the extractor has to learn to make it difficult to distinguish domains. The equation for backpropagation is as follows:

$$\theta_f \leftarrow \theta_f - \mu \left( \frac{\partial \mathcal{L}_y^i}{\partial \theta_f} - \lambda_p \frac{\partial \mathcal{L}_D^i}{\partial \theta_f} \right) \quad (6)$$

$$\theta_y \leftarrow \theta_y - \mu \frac{\partial \mathcal{L}_y^i}{\partial \theta_f} \quad (7)$$

$$\theta_d \leftarrow \theta_d - \mu \lambda_p \frac{\partial \mathcal{L}_D^i}{\partial \theta_f} \quad (8)$$

where  $\theta_f$  is the parameters of the feature extractor,  $\theta_y$  is the parameters of the predictor,  $\theta_d$  is the parameters of the discriminator,  $\mu$  is the learning rate, and  $\lambda_p$  is the scheduling parameter.

If the domain classification loss is backpropagated with a large value before the algorithm classifies the class well, the extractor prevents clustering of the same class. To avoid this situation, the extractor slowly backpropagates the domain classification loss through the following hyper-parameter:

$$\lambda_p = \frac{2}{1 + \exp(-\gamma \cdot p)} - 1 \quad (9)$$

where  $\gamma$  is the hyper-parameter of the domain adaptation, and  $p$  is the training progress.

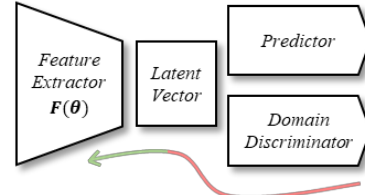


Figure 6. Schematic illustration of the domain adversarial neural network.

### 3.3. Maximum Mean Discrepancy (MMD)

MMD is also used to better solve the domain-shift problem between the source and target data (Borgwardt, Gretton, Rasch, Kriegel, Schölkopf, Karsten & Smola, 2006). It is graphically described in Figure 7. The latent space from the feature extractor is a high-dimensional vector. If the distribution of the same class in a high-dimensional space is similar, it means that the features are extracted well, regardless of the domain. MMD is used to reduce the distribution discrepancy. The distribution difference between the source and the target domains is calculated by mapping the high-dimensional features into Reproducing Kernel

Hilbert Space (RKHS). The loss function to minimize the MMD between the domains is defined as follows:

$$\mathcal{L}_{MMD} = \left\| \frac{1}{m^s} \sum_{i=1}^{m^s} \phi \left( F \left( \chi_S^{(i)} \right) \right) - \frac{1}{m^T} \sum_{i=1}^{m^T} \phi \left( F \left( \chi_T^{(i)} \right) \right) \right\|_{\mathcal{H}}^2 \quad (10)$$

where  $\chi_S$  is input data of the source domains,  $\chi_T$  is the input data of the target domain,  $F$  is the feature extractor, and  $\phi$  is a mapping function. This paper uses the gaussian kernel, from among the kernels that satisfy the RKHS, as the mapping function. The proposed method uses five source domains and one target domain. To adapt the target domain to the multi-source domain, the sample of the target domain is increased by five times during the training process. By slightly modifying the existing MMD method, the proposed method calculated the MMD value between five source domains and the target domain with samples copied five times.

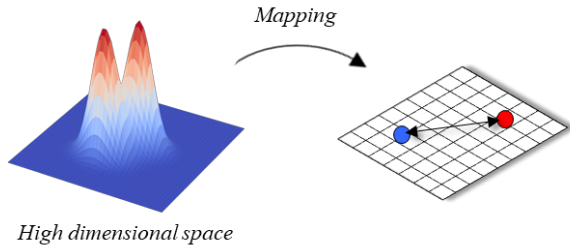


Figure 7. Concept of maximum mean discrepancy.

### 3.4. Ensemble Learning

The performance of a deep-learning model changes across various situations, including the initialization distribution, even for the same model. For this reason, the proposed model uses an ensemble method that uses soft voting to reduce uncertainty.  $N$  models are trained with different random seeds to consider the uncertainty due to the parameter initialization;  $N$  is set as five in this work. First, the sum of the output values of the predictor based on  $N$  models is obtained. Then, the label with the maximum value is selected. It is graphically described in Figure 8. The equation for the ensemble is as follows:

$$y = \underset{y}{\operatorname{argmax}} \left( \sum_{i=0}^N P(F(\chi_i)) \right) \quad (11)$$

where  $P$  is the predictor, and  $N$  is the number of models.

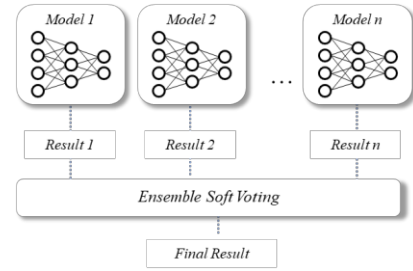


Figure 8. Soft-voting-based ensemble method.

## 4. EXPERIMENTAL VALIDATION

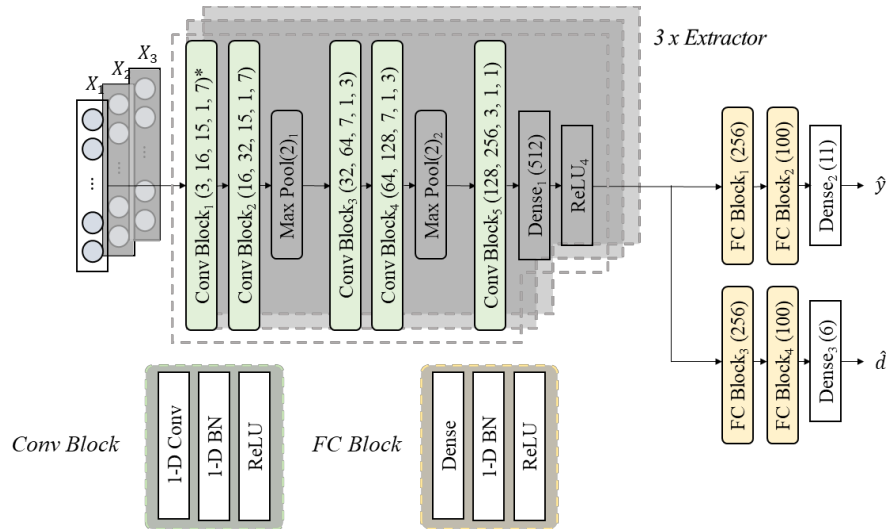


Figure 9. The model architecture of the proposed method.

The model architecture of the proposed method is described in Figure 9. The length of input data ( $\chi$ ) is 300, and the

number of channels is 3. A convolutional neural network (CNN) was used to construct the three feature extractors as

each input for the three preprocessed crops. The extractor is composed of five convolutional blocks, two max-pool layers, and one dense layer. The convolutional block consists of a one-dimensional convolutional layer, a batch normalization layer, and a rectified linear unit (ReLU). Then, the extractor has a 512-dimensional latent vector as an output. The fully connected (FC) block consists of a dense layer, a batch normalization layer, and a ReLU. The predictor and the domain discriminator consist of two FC blocks and one dense layer. In determining the optimal parameters for the proposed method, various methods were employed. The kernel size of the extractor was selected through a grid search, evaluating a range of sizes, including 3, 5, 7, 15, and 25. On the other hand, the configuration of the predictor and domain discriminator - specifically, the number of layers and neurons - was established manually. The number of channels was set to double with each successive layer. Moreover, the number of layers was tuned manually, employing a strategy that involved incrementally adding or subtracting a single layer at a time. The epoch was set as 100 and the batch size was

**Input:** Labeled pressure signal samples from source dataset  $\mathcal{D}_S = \{\mathbf{X}_s, y_s\}$ , unlabeled pressure signal samples from target dataset  $\mathcal{D}_T = \{\mathbf{X}_T\}$ , batch size  $b$ , training epoch  $epochs$ , learning rate  $\mu$

**Output:** Configuration of the proposed method

I) Randomly initialize the parameters

II) Train the model

**for** epoch = 1 **to**  $epochs$  **do**

**for** batch = 1 **to** number of batches **do**

1) Sample mini-batch  $\{\chi_s^{(i)}, y_s^{(i)}\}_{i=1}^b$  and  $\{\chi_T\}_{i=1}^b$

2) Forward propagation

Calculate the output of the three feature extractor  $F_1(\chi_s^{(i)})$ ,  $F_1(\chi_T^{(i)})$ ,  $F_2(\chi_s^{(i)})$ ,  $F_2(\chi_T^{(i)})$ ,  $F_3(\chi_s^{(i)})$ ,  $F_3(\chi_T^{(i)})$  and combine each features

Calculate the output of predictor  $\hat{y}^{(i)}$

Calculate the output of discriminator  $\hat{d}^{(i)}$

Calculate the objective function  $\mathcal{L} = \mathcal{L}_y + \alpha \mathcal{L}_D + \beta \mathcal{L}_{MMD}$

3) Backpropagation by Adam optimization

$$\theta_f \leftarrow \theta_f - \mu \left( \frac{\partial \mathcal{L}_y^i}{\partial \theta_f} - \lambda_p \frac{\partial \mathcal{L}_D^i}{\partial \theta_f} \right)$$

$$\theta_y \leftarrow \theta_y - \mu \frac{\partial \mathcal{L}_y^i}{\partial \theta_f}$$

$$\theta_d \leftarrow \theta_d - \mu \lambda \frac{\partial \mathcal{L}_D^i}{\partial \theta_f}$$

**end for**

**end for**

III) Predict the label on the target dataset  $\mathcal{D}_T = \{\chi_T\}_{i=1}^b$

Algorithm 1. Training procedure

chosen as 128. The penalty parameters  $(\alpha, \beta)$  were empirically selected as (1, 1). Five models were used for the soft-voting-based ensemble. The training was conducted on a computer with a CPU with an Intel(R) Xeon(R) Gold 5218R CPU@2.10GHz and a GPU with an NVIDIA RTX A6000. The software environment used was Python 3.7 and PyTorch 1.12.0. The pseudo code of the training process is shown in Algorithm 1.

#### 4.1. Results from the Validation Dataset

The accuracy of the proposed method, when applied to individual dataset 3 was 100.00%. Figure 10 shows the latent vector of one model for the validation dataset through t-SNE (t-distributed Stochastic Neighbor Embedding) (Van der Maaten & Hinton, 2008). Circles indicate source data and triangles indicate target data. Also, color is used to distinguish each class, and the class for the target data is shown as the label predicted by the predictor. As can be seen from the figure, the source and target features overlap with each other. This means that the extractor of the proposed method extracts domain-invariant features.

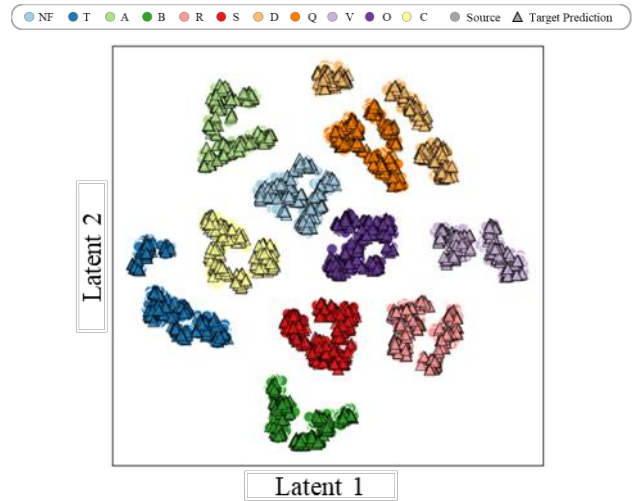


Figure 10. t-SNE visualization of the validation dataset (individual dataset 3).

#### 4.2. Test Dataset Result

The accuracy of the proposed method, when applied to individual datasets 7 and 8, was 99.77%; this result allowed the proposed approach to rank in 2<sup>nd</sup> place in the 2022 PHM Conference Data Challenge. Figure 11 presents the t-SNE visualization of the features extracted by the proposed method; the graphical description of the figure is the same as that in Figure 10. Although the source data and the target data overlap, it can be seen that the domain shift still exists, when

compared to the validation dataset. This is because the difference between the training dataset and the test dataset is large.

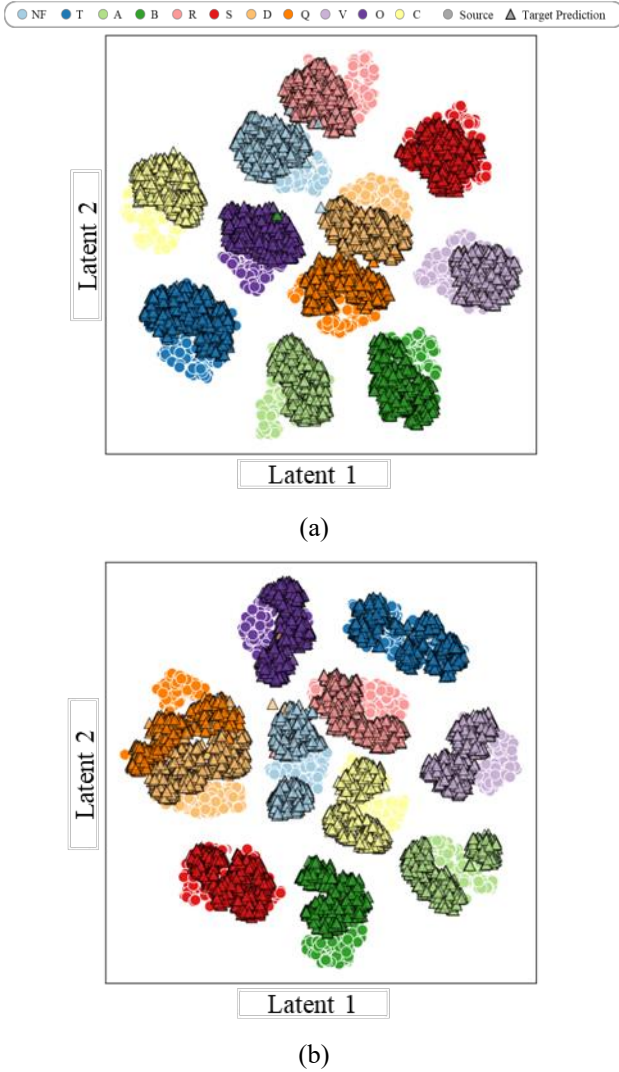


Figure 11. t-SNE visualization of the test datasets: (a) individual dataset 7, and (b) individual dataset 8.

### 4.3. Discussion for Result

Two additional studies were performed to verify the proposed method with a validation dataset; A penalty parameter study was performed in Section 4.3.1, and an ablation study was conducted in Section 4.3.2.

#### 4.3.1. Penalty parameter study

In Eq. (2), the proposed method has three loss functions: task classification loss ( $\mathcal{L}_y$ ), domain classification loss ( $\mathcal{L}_D$ ), and MMD loss ( $\mathcal{L}_{MMD}$ ). The penalty parameters  $\alpha$  and  $\beta$  are

weighted according to the importance of the loss function. We performed a penalty parameter study on the validation dataset without applying the ensemble method. Table 4 shows the results, showing 100% accuracy for a total of 5 combinations. When  $\alpha$  or  $\beta$  equals 10, low performance is shown, and high performance is shown when  $\alpha$  and  $\beta$  have the same value. In addition, it can be seen that the proposed method does not significantly affect the performance when  $\alpha$  and  $\beta$  are less than 1.

Accuracy (%)	$\alpha = 0.001$	$\alpha = 0.01$	$\alpha = 0.1$	$\alpha = 1$	$\alpha = 10$
$\beta = 0.001$	99.81	97.27	<b>100</b>	98.34	96.61
$\beta = 0.01$	99.91	<b>100</b>	<b>100</b>	96.14	95.67
$\beta = 0.1$	99.12	99.97	99.84	99.75	93.88
$\beta = 1$	99.78	<b>100</b>	98.84	<b>100</b>	96.58
$\beta = 10$	93.81	94.03	95.10	98.49	94.25

Table 4. Penalty parameter study for the validation dataset

#### 4.3.2. Ablation study

An ablation study was performed to verify the proposed method. We performed three comparative models without applying the ensemble method, and the description of the models is as follows:

1. w/o data cropping technique: A model that does not use the data cropping technique described in Section 3.1; Only the center part with a length of 300 was used.
2. w/o adversarial learning: A model that does not use adversarial learning of the domain adversarial neural network described in Section 3.2
3. w/o MMD: A model that does not use the loss function that minimizes the maximum mean discrepancy for multi-source described in Section 3.3

The accuracy decreased slightly when adversarial learning or MMD was not used, but the accuracy decreased by 2.73% when the data cropping technique was not used. This shows that the data crop preprocessing technique using physical knowledge in the proposed method has the most important effect on performance.

Method	Accuracy (%)
w/o data crop technique	97.27
w/o adversarial learning	99.47
w/o MMD	99.5
Proposed method	<b>100</b>

Table 3. Ablation study for the validation dataset

## 5. CONCLUSION

In this paper, we proposed a new domain-adaptation-based fault-diagnosis approach to solve the domain-shift issue that arises due to the variable operating conditions of a rock drill. A data cropping technique was employed to mitigate the different impact cycles of a rock drill. The proposed method combines a domain adversarial neural network and maximum mean discrepancy to solve the domain-shift issue. In addition, a soft-voting-based ensemble was introduced to reduce the model uncertainty. The proposed method achieves outstanding performance on the validation and test datasets and was ranked in 2<sup>nd</sup> place in the 2022 PHM Conference Data Challenge.

## ACKNOWLEDGEMENT

This research was financially supported by the Ministry of Trade, Industry and Energy (MOTIE) and Korea Institute for Advancement of Technology (KIAT) through the International Cooperative R&D program (Project No. P0011923) and HRD Program for Industrial Innovation (Project No. P0008691).

## NOMENCLATURE

$m$	Batch size
$\mu$	Learning rate
$\chi$	Preprocessed signal
$y$	Label of the health condition
$\hat{y}$	Predicted label of the class
$d$	Label of the domain
$\hat{d}$	Predicted label of the domain
$\theta_f$	Parameter of the feature extractor
$\theta_y$	Parameter of the classifier
$\theta_d$	Parameter of the domain discriminator
$\lambda_p$	Scheduling parameter
$\gamma$	Hyper-parameter of the domain adaptation
$p$	Training progress
$\phi$	Mapping function

## REFERENCES

- Erik, J., Erik, F., Mattias, K., & Robert, P. (2021). Fault Identification in Hydraulic Rock Drills from Indirect Measurement During Operation. *IFAC-PapersOnLine*, vol. 54(11), pp. 73-78. doi.org/10.1016/j.ifacol.2021.10.053
- Li, B., Chow, MY., Tipsuwan, Y., & Hung, J.C. (2000) Neural-network-based motor rolling bearing fault

- diagnosis. *IEEE transactions on industrial electronics*, vol.47(5), pp. 1060-1069. doi.org/10.1109/41.873214
- Guo, X., Chen, L., & Shen, C. (2016). Hierarchical adaptive deep convolution neural network and its application to bearing fault diagnosis. *Measurement*, vol. 93, pp. 490-502. doi.org/10.1016/j.measurement.2016.07.054
- Ganin, Y., Ustinova, E., Ajakan, H., Germain, P., Larochelle, H., Laviolette, F., Marchand, M., & Lempitsky, V. (2016). Domain-adversarial training of neural networks. *The journal of machine learning research*, vol.17(1), pp. 2096-2030. doi.org/10.48550/arXiv.1505.07818
- Jiao, J., Zhao, M., & Lin, J. (2019). Unsupervised adversarial adaptation network for intelligent fault diagnosis. *IEEE Transactions on Industrial Electronics*, vol. 67(11), pp. 9904-9913. doi.org/10.1109/TIE.2019.2956366
- Guo, L., Lei, Y., Xing, S., Tan, T., & Li, N. (2018). Deep convolutional transfer learning network: A new method for intelligent fault diagnosis of machines with unlabeled data. *IEEE Transactions on Industrial Electronics*, vol.66(9) pp. 7316-7325. doi.org/10.1109/TIE.2018.2877090
- Borgwardt, KM., Gretton, A., Rasch, MJ., Kriegel, HP., Schölkopf, B., Karsten M., & Smola, AJ. (2006) Integrating structured biological data by kernel maximum mean discrepancy. *Bioinformatics*, vol.22(14) pp. 49-57. doi.org/10.1093/bioinformatics/btl242
- Van der Maaten, L., & Hinton, G., (2008). Visualizing data using t-SNE. *Journal of machine learning research*, 9 (11).

## BIOGRAPHIES



**Yong Chae Kim** received the B.S. degree in mechanical engineering from Yonsei University, Seoul, South Korea, in 2022. He is currently pursuing the M.S. in the Department of Mechanical Engineering at Seoul National University, Seoul, South Korea. His research interests include machine learning and deep learning for diagnostics of rotating machinery.



**Taehun Kim** received the B.S. degree in mechanical engineering from Hanyang University, South Korea, in 2021. He is currently pursuing the M.S. degree in the Department of Mechanical Engineering at Seoul National University, South Korea. His research interests include machine learning and deep learning for the diagnosis of rotating machinery.



**Jin Uk Ko** received a B.S. degree in mechanical engineering from Seoul National University, Seoul, South Korea, in 2017. He is currently pursuing a Ph.D. degree in the Department of Mechanical Engineering at Seoul National University, Seoul, South Korea. His research interests include machine learning and deep learning for anomaly detection and diagnostics of rotating machinery.



**Jinwook Lee** received the B.S. degree in mechanical engineering from Hanyang University, Seoul, South Korea, in 2019. He is currently pursuing a Ph.D. degree in the Department of Mechanical Engineering at Seoul National University, Seoul, South Korea. His research interests include machine learning and deep learning for diagnostics of rotating machinery.



**Keon Kim** received the B.S. degree from Korea Aerospace University, Goyang-si, South Korea, in 2009, in material science, and the M.S. degree from Seoul National University, Seoul, in 2017, where he is currently working toward the Ph.D. degree in the Department of Mechanical and Aerospace Engineering. He has been working at Hyundai Doosan Infracore Co., Ltd., a construction machinery company, since 2009. His doctoral research topic is prognostics and health management for earthmoving machinery.